Acceleration of conduction velocity linked to clustering of nodal components precedes myelination

Sean A. Freeman[a,b,c,1], Anne Desmazières[a,b,c,1], Jean Simonnet[a,b,c], Marie Gatta[a,b,c], Friederike Pfeiffer[a,b,c], Marie Stéphane Aigrot[a,b,c], Quentin Rappeneau[a,b,c], Serge Guerreiro[a,b,c], Patrick Pierre Michel[a,b,c], Yuchio Yanagawa[d,e], Gilles Barbin[a,b,c], Peter J. Brophy[f], Desdemona Fricker[a,b,c], Catherine Lubetzki[a,b,c,g,1,2], and Nathalie Sol-Foulon[a,b,c,1,2]

[a]Sorbonne Universités Université Pierre et Marie Curie University of Paris 06, UMR_S 1127, Institut du Cerveau et de la Moelle–Groupe Hospitalo-Universitaire Pitié-Salpêtrière, F-75013, Paris, France; [b]INSERM U1127, F-75013, Paris, France; [c]CNRS UMR7225, F-75013, Paris, France; [d]Department of Genetic and Behavioral Neuroscience, Gunma University Graduate School of Medicine, Maebashi 371-8511, Japan; [e]Japan Science and Technology Agency, Tokyo 102-8666, Japan; [f]Centre for Neuroregeneration, University of Edinburgh, Edinburgh EH16 ASB, United Kingdom; and [g]Assistance Publique-Hôpitaux de Paris, Hôpital Pitié-Salpêtrière, 75013, Paris, France

Edited by William A. Catterall, University of Washington School of Medicine, Seattle, WA, and approved December 16, 2014 (received for review October 6, 2014)

High-density accumulation of voltage-gated sodium (Na_v) channels at nodes of Ranvier ensures rapid saltatory conduction along myelinated axons. To gain insight into mechanisms of node assembly in the CNS, we focused on early steps of nodal protein clustering. We show in hippocampal cultures that prenodes (i.e., clusters of Na_v channels colocalizing with the scaffold protein ankyrinG and nodal cell adhesion molecules) are detected before myelin deposition along axons. These clusters can be induced on purified neurons by addition of oligodendroglial-secreted factor(s), whereas ankyrinG silencing prevents their formation. The Na_v isoforms $Na_v1.1$, $Na_v1.2$, and $Na_v1.6$ are detected at prenodes, with $Na_v1.6$ progressively replacing $Na_v1.2$ over time in hippocampal neurons cultured with oligodendrocytes and astrocytes. However, the oligodendrocyte-secreted factor(s) can induce the clustering of $Na_v1.1$ and $Na_v1.2$ but not of $Na_v1.6$ on purified neurons. We observed that prenodes are restricted to GABAergic neurons, whereas clustering of nodal proteins only occurs concomitantly with myelin ensheathment on pyramidal neurons, implying separate mechanisms of assembly among different neuronal subpopulations. To address the functional significance of these early clusters, we used single-axon electrophysiological recordings in vitro and showed that prenode formation is sufficient to accelerate the speed of axonal conduction before myelination. Finally, we provide evidence that prenodal clusters are also detected in vivo before myelination, further strengthening their physiological relevance.

node of Ranvier | sodium channel | myelination | GABAergic neuron | conduction velocity

Voltage-gated sodium (Na_v) channels are highly enriched at the axon initial segment (AIS) and the node of Ranvier, allowing generation and rapid propagation of action potentials by saltatory conduction in myelinated fibers. These axonal domains also contain cell adhesion molecules [e.g., neurofascin 186 (Nfasc186)] and the scaffolding proteins ankyrinG (AnkG) and βIV spectrin, which provide a potential link with the actin cytoskeleton (1). Flanking the nodes are the paranodes, where axoglial junctions between paranodal myelin loops and the axon are formed through interactions between axonal contactin-associated protein (Caspr)/contactin and glial Nfasc155 (2, 3). Although the mechanisms of nodal assembly are best characterized in the peripheral nervous system (4–9), less is known about the cellular and molecular mechanisms underlying node assembly in the CNS. ECM proteins, adhesion molecules, such as Nfasc186, and also, axoglial paranodal junctions have been shown to trigger CNS nodal clustering, although their respective roles remain uncertain (10–19). Moreover, axonal clustering of Na_v channels before myelin deposition and oligodendroglial contact has been shown to occur in retinal ganglion cell (RGC) cultures, where these clusters were induced by oligodendroglial-secreted factor(s) (20, 21).

Here, we have investigated the cellular and molecular mechanisms underlying nodal protein assembly in hippocampal neuron cultures. We first showed that evenly spaced clusters of Na_v channels, colocalizing with Nfasc186 and AnkG, are detected along axons before myelination. Strikingly, this prenode assembly is restricted to GABAergic interneurons, suggesting the existence of different mechanisms of nodal assembly. The prenodal clustering can be induced on purified neurons by the addition of oligodendroglial-secreted factor(s) and also depends on intrinsic cues, such as AnkG. Furthermore, we also provide evidence that these clusters are detected in vivo before myelination on hippocampal tissue sections. Finally, to gain insight into their functional significance, we performed in vitro simultaneous somatic and axonal recordings and showed that the presence of prenodes increases the speed of action potential propagation along axons before myelination.

Results

Clusters of Nodal Proteins Are Detected Before Myelination on Hippocampal GABAergic Axons. To gain insight into the chronology of axonal domain assembly, we first analyzed the distribution of Na_v channels in mixed hippocampal cultures (i.e., neurons with oligodendrocytes and astrocytes) from embryonic day 18 (E18) rat embryos at different time points before myelination.

Significance

Cellular and molecular mechanisms underlying the assembly of nodes of Ranvier of myelinated axons in the CNS are still only partly understood. Our study shows the influence of intrinsic cues and glial extrinsic factors for nodal protein clustering before myelination on specific hippocampal neuronal subpopulations and extends to electrophysiological understandings and in vivo relevance. Although conduction velocity along axons has long been thought to mostly rely on the insulating properties of myelin, we here show that nodal protein aggregation can increase this speed in the absence of such insulation. These results highlight the role of nodal clusters per se on conduction velocity by uncoupling it from myelination.

Author contributions: S.A.F., A.D., J.S., G.B., D.F., C.L., and N.S.-F. designed research; S.A.F., A.D., J.S., M.G., F.P., M.S.A., Q.R., S.G., and N.S.-F. performed research; P.P.M., Y.Y., and P.J.B. contributed new reagents/analytic tools; S.A.F., A.D., J.S., D.F., C.L., and N.S.-F. analyzed data; and S.A.F., A.D., C.L., and N.S.-F. wrote the paper.

The authors declare no conflict of interest.

This article is a PNAS Direct Submission.

[1]S.A.F., A.D., C.L., and N.S.-F. contributed equally to this work.

[2]To whom correspondence may be addressed. Email: catherine.lubetzki@psl.aphp.fr or nathalie.sol-foulon@upmc.fr.

This article contains supporting information online at www.pnas.org/lookup/suppl/doi:10.1073/pnas.1419099112/-/DCSupplemental.

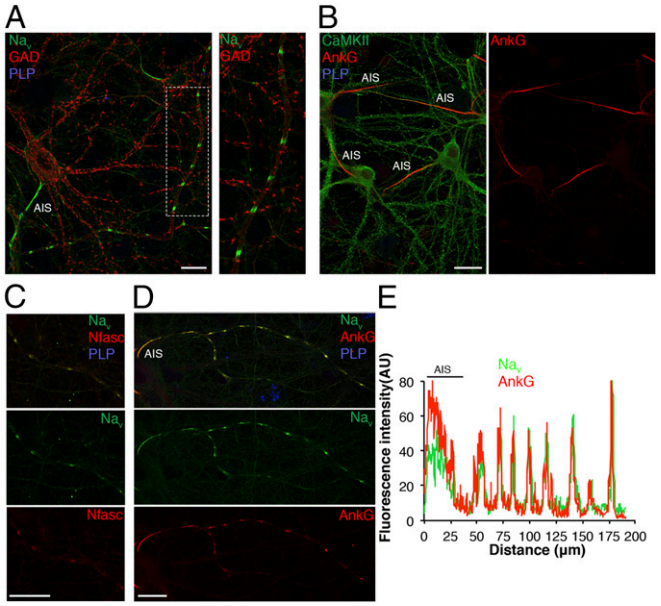

Fig. 1. Prenodes are formed before myelination on hippocampal GABAergic neurons in culture. Immunostaining of mixed hippocampal rat cultures at 17 DIV. (*A*) Clustering of Na_v (green) in the absence of myelin (PLP^-; blue) along a GABAergic axon ($GAD67^+$; red), (*B*) contrasting with the absence of prenodal clusters (AnkG; red) on the axons of pyramidal cells Ca^{2+}/calmodulin-dependent protein kinase II^+ ($CaMKII^+$; green). Na_v clusters (green) colocalized with (*C*) Nfasc186 (Nfasc) and (*D*) AnkG (plot profile is in *E*) in red along unmyelinated axons (PLP^-; blue). (Scale bars: 25 μm.)

Hippocampal neuronal cultures contain both glutamatergic pyramidal cells, identified by Ca^{2+}/calmodulin-dependent protein kinase II immunolabeling (75% ± 5% of neurons), and GABA releasing interneurons, identified by glutamate decarboxylase isoform of 67 kDa (GAD67) expression (24.5% ± 3.9% of neurons). As might be predicted, Na_v channel accumulation was detected at the AIS of all neurons during the first week of culture and colocalized with AnkG and Nfasc186, whereas expression along the axon was diffuse and barely visible. Surprisingly, in contrast, at 17 days in vitro (DIV), evenly spaced clusters of Na_v channels AnkG and Nfasc186 were found exclusively localized on GABAergic neurons (67% ± 15% of total $GAD67^+$ neurons) (Fig. 1 and Fig. S1). These clusters, which were formed in the absence of myelin ensheathment as indicated by the lack of proteolipid protein (PLP) immunostaining (Fig. 1 *A*, *C*, and *D*), were named prenodes. The percentage of hippocampal axons with prenodes increased as a function of time in vitro from 4.1% ± 3.1% at 14 DIV to 15.8% ± 3.5% and 17.1% ± 7.1% at 17 and 21 DIV, respectively. We also observed that the number of prenodes distributed along each axon increased from 14 to 21 DIV (Fig. S1*B*).

Because hippocampal interneurons are highly diverse (22), we further investigated whether neurons with prenodes are restricted to a particular interneuron subtype by characterizing calcium-binding protein (i.e., calbindin, calretinin, and parvalbumin) and somatostatin expression. Most neurons with prenodes were $somatostatin^+$ and/or $parvalbumin^+$ (81.3% ± 6.8% and 57.5% ± 3.5, respectively) (Fig. S2), suggesting an overlap in prenodal formation between varying interneuron subtypes, particularly those that express both somatostatin and parvalbumin together (23).

Prenode Assembly Requires Oligodendroglial Cues. To gain insight into the role of glial cells in prenode formation, we used purified hippocampal neuronal cultures through elimination of dividing cells by antimitotic treatment, which were virtually devoid of oligodendrocytes and contained a small percentage of astrocytes (less than 5%). We observed that purified neurons with nodal protein clusters along axons were rare (1.1% ± 0.7%) (Fig. 2 *A* and *F*). However, when we prepared highly purified populations of oligodendroglial lineage cells and added oligodendrocytes or oligodendroglial-conditioned medium (OCM) to purified neuronal cultures, the percentage of axons with prenodes increased, respectively from 1.1% ± 0.7% to 10.8% ± 3.3% and 11.9% ± 3.9% (Fig. 2*F*). Under these conditions, Na_v was observed to colocalize with AnkG and Nfasc186 in prenodes (Fig. 2 *B* and *D*). Furthermore, similar to mixed cultures, prenodes were restricted to $GAD67^+$ neurons (Fig. 2*C*). The number of prenodes along each axon was decreased compared with mixed cultures (Fig. S1*C*), and the spacing between clusters was shorter in OCM-treated purified neurons compared with neurons in mixed cultures (9.6 ± 1.1 and 15.8 ± 1.8 μm, respectively; $P = 0.028$) (Fig. 2*E*). In addition, nodal protein clustering occurred preferentially along axons with highly phosphorylated neurofilaments, suggesting an association with neuronal maturity (Fig. 2*D*). Altogether, our results show that glial cues are necessary and that a diffusible oligodendroglial factor(s) participate(s) in prenode formation along GABAergic axons.

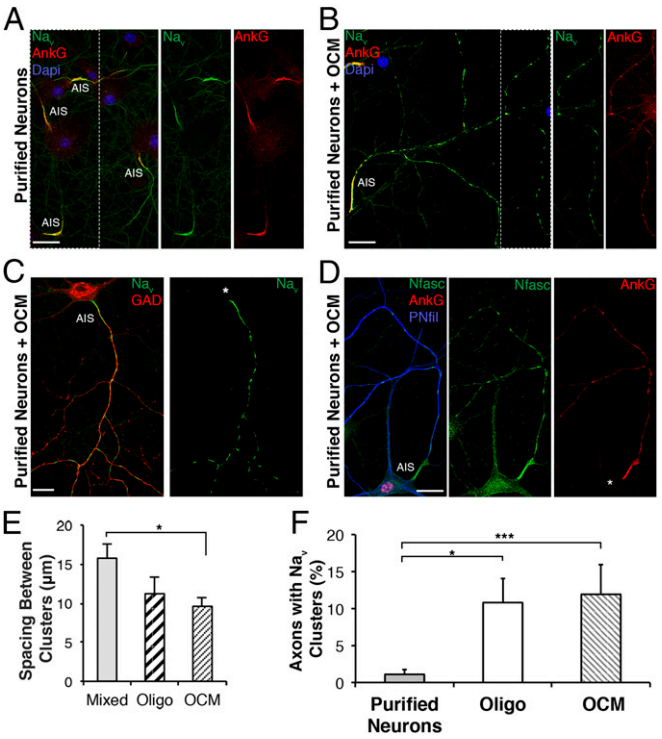

Fig. 2. A secreted oligodendroglial factor promotes nodal protein clustering. Immunostaining of purified hippocampal neurons cultured in the (*A*) absence or (*B–D*) presence of OCM. (*A–D*) The AIS is detected in all conditions, but (*B–D*) clusters of Na_v (green), AnkG (red), and Nfasc (green) are only detected in the presence of OCM. (*C*) Prenodes are formed on $GAD67^+$ neurons treated with OCM. (*D*) Neuronal cell body and neurites stained with an Ab targeting phosphorylated neurofilaments (PNfil; blue). (Scale bars: 25 μm.) (*E*) Distance between prenodes measured on axons in mixed culture or purified neurons cocultured with oligodendrocytes (oligo) or OCM. Mean spacing between clusters (micrometers) ± SEM of four independent experiments is shown. *$P = 0.028$ (Mann–Whitney test). (*F*) Percentage of axons (AIS^+) having at least two Na_v clusters at 21 DIV in purified neuron cultures, purified neurons cocultured with oligodendrocytes (oligo), or OCM. The means ± SDs of 4 (for oligo) and 10 (for OCM) independent experiments are shown. For each experiment, at least 100 neurons were analyzed. *$P = 0.0187$; ***$P = 0.0003$ (Mann–Whitney test).

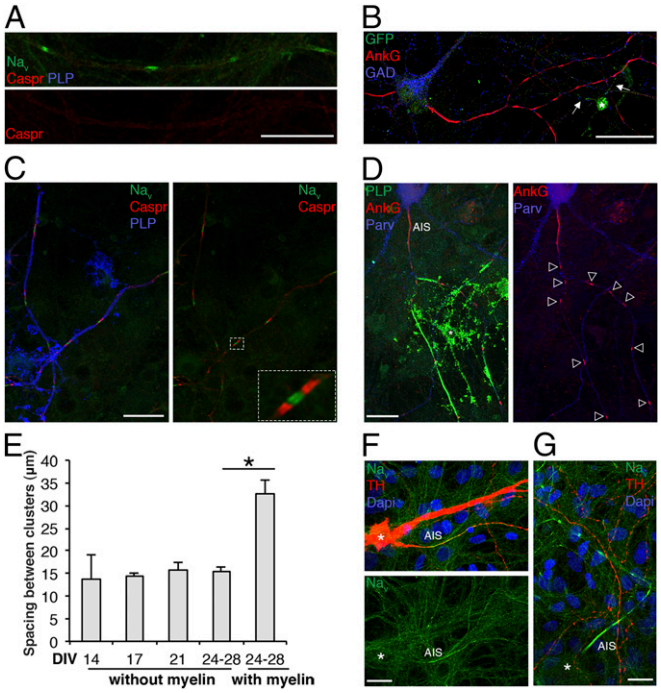

Fig. 3. Prenodes are formed on myelin-competent GABAergic neurons. (*A* and *B*) Immunostaining of mixed hippocampal culture at 17 DIV. (*A*) Na_v clusters (green) observed in the absence of Caspr aggregation (red) and the absence of myelin (PLP^-; blue). (*B*) Hippocampal culture from *CNP-EGFP* embryos shows an oligodendrocyte (asterisk) stained with an anti-GFP Ab with processes contacting the axon (arrows). Numerous AnkG clusters (red) are observed at a distance from these processes on a $GAD67^+$ neuron (blue). (*C* and *D*) Immunostaining of mixed hippocampal culture at 24 DIV. (*C*) Myelinated axons (PLP^+; blue) with nodes (Na_v; green) and paranodes (Caspr; red). A higher magnification of a node with flanking paranodes is shown. (*D*) Myelinated segments (PLP^+; green) with nodes ($AnkG^+$; red) on GABAergic axons [$Parvalbumin^+$ (Parv); blue]. (Scale bars: 25 μm.) (*E*) Measure of the distance between prenodes on unmyelinated axons and between nodes of Ranvier on myelinated axons at different time points. Values are the mean spaces between clusters (micrometers) ± SEMs of four independent experiments. *$P = 0.028$ (Mann–Whitney test). (*F* and *G*) Immunostaining of mesencephalic cultures at 21 DIV. (*F*) Dopaminergic neurons tyrosine hydroxylase (TH^+; red) do not form Na_v clusters downstream of the AIS (Na_v^+; green), whereas (*G*) Na_v clusters are formed on a nondopaminergic (TH^-) axon. *Neuronal cell body. (Scale bars: 25 μm.)

Hippocampal GABAergic and Pyramidal Neurons Assemble Nodal Proteins by Different Mechanisms. To further examine if oligodendrocytes were contacting prenodes, we used mixed hippocampal cultures from *CNP-EGFP* embryos, in which all cells in the oligodendrocyte lineage express EGFP (24). Although oligodendrocyte processes contacted some axons with prenodes, most clusters were not (Fig. 3*B*), suggesting that nodal protein clustering on GABAergic interneurons does not depend on strict oligodendroglial contact. In addition, prenodes were formed independently of paranodal aggregation as indicated by the diffuse Caspr expression (Fig. 3*A*).

We also examined, at later time points (24–28 DIV), whether neurons were eventually myelinated by analyzing mixed hippocampal cultures treated with differentiation medium to enhance the myelination process. Myelinated axons were detected with Na_v channel clusters flanked by paranodal Caspr clusters, forming either heminodes or nodes of Ranvier at the tips of myelinated internodes (Fig. 3*C*). Myelinated internodes were detected on both GABAergic and pyramidal neurons (Fig. 3*D* and Fig. S3), suggesting that clustering at the node on glutamatergic axons coincides with myelin deposition, in contrast to GABAergic axons. Within GABAergic myelinated axons, internodal length was 32.7 ± 3.1 μm (i.e., twofold longer than the distance between clusters observed in nonmyelinated GABAergic axons present at the same time point in the same cultures) (Fig. 3*E*). To determine if prenodal clustering is restricted to neurons destined to be myelinated, we used dopaminergic neurons in culture, which are known to remain unmyelinated in vivo. These neurons exhibited Na_v clustering at the AIS but not along axons (Fig. 3 *F* and *G*).

Taken together, our results suggest that the mechanisms of nodal assembly differ between neuron subtypes. Indeed, whereas most GABAergic neurons assemble prenodes before myelination, hippocampal pyramidal cells initiate nodal clustering concomitantly to myelination.

Na_v Channel Isoforms Are Differentially Regulated in Prenodes over Time in Vitro. Because CNS nodes of Ranvier express different Na_v α-subunits (25, 26), we also analyzed prenodal expression of Na_v α-subunits before myelination. $Na_v1.1$ was detected in more than 90% of $AnkG^+$ clusters at all time points analyzed (Fig. 4*D*), whereas $Na_v1.2$ was mainly detected at 14 DIV (Fig. 4) and progressively disappeared at later time points. $Na_v1.6$, which

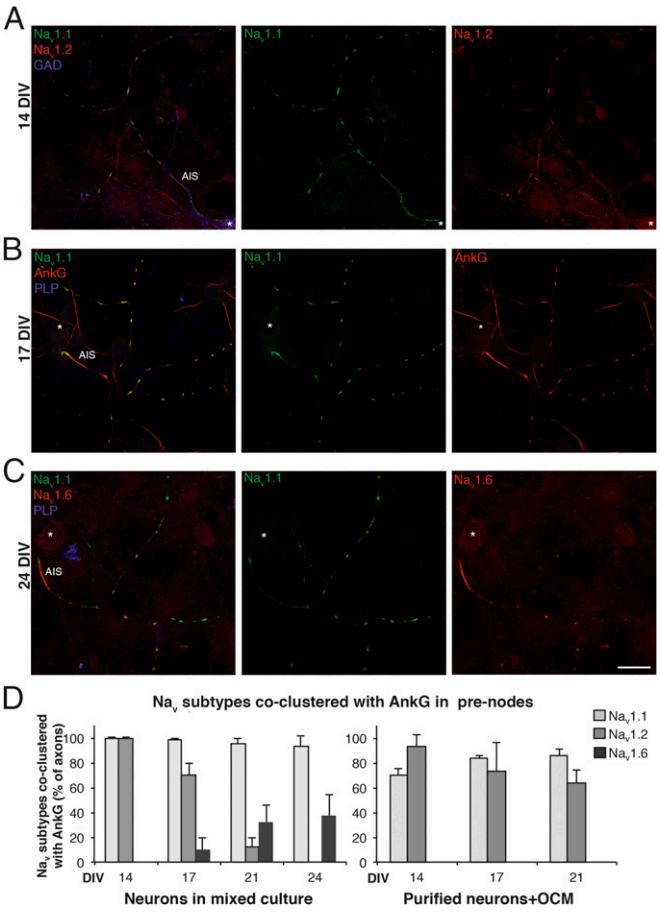

Fig. 4. Prenodes express different Na_v isoforms. (*A*–*C*) Hippocampal neuron cultures at (*A*) 14, (*B*) 17, or (*C*) 24 DIV immunostained for $Na_v1.1$, $Na_v1.2$, $Na_v1.6$, AnkG, GAD, and/or PLP as indicated, illustrating the different Na_v α-subunit isoform expression in prenodes at different time points. *Neuronal cell body. (Scale bar: 25 μm.) (*D*) Percentage of axons with clusters of AnkG, which are colocalized with $Na_v1.1$, $Na_v1.2$, or $Na_v1.6$ at different DIVs. Quantifications were performed in mixed cultures and cultures of purified neurons with OCM. The means ± SDs of three independent experiments are shown. For each experiment, at least 100 neurons were analyzed.

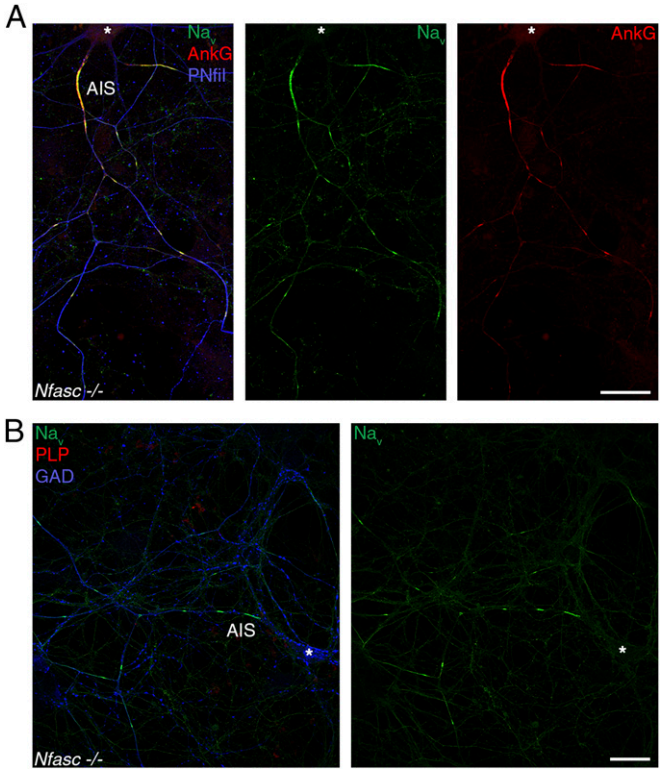

Fig. 5. Prenodes are formed in the absence of Nfasc expression. Immunostaining of hippocampal neuron cultures of *Nfasc*$^{-/-}$ mice at 20 DIV showing clusters of Na_v (green) and AnkG (red) along an axon with phosphorylated neurofilaments (PNfil; blue) in *A* and in the absence of myelin (PLP^{-}; red) on a GAD67^{+} neuron (blue) in *B*. *Neuronal cell body. (Scale bars: 25 μm.)

appeared at 17 DIV, was detected at 21 DIV before myelination on 32.2% ± 13.3% of axons with prenodes (Fig. 4 *B* and *D*). In contrast, in pure hippocampal neuronal cultures treated with OCM, whereas $Na_v1.1$ and/or $Na_v1.2$ were expressed in prenodes, $Na_v1.6$ was not detected (Fig. 4*D*). These results show that Na_v channel isoforms described at nodes of Ranvier in myelinated fibers (26) are expressed in prenodal clusters on unmyelinated fibers in hippocampal cultures. Moreover, oligodendrocyte-secreted factors can induce the clustering of $Na_v1.1$ and $Na_v1.2$ but not $Na_v1.6$ isoforms in prenodes.

Nfasc Is Not Necessary for Prenode Assembly. In the CNS, Nfasc186 can induce nodal clustering of Na_v channels in the absence of intact paranodal junctions (19), and it has been proposed recently that Nfasc186 participates in nodal protein clustering in the presence of nodal ECM molecules (12). To address the role of Nfasc186 as the neuronal organizer of prenodes, we prepared mixed hippocampal cultures from *Nfasc*$^{-/-}$ or WT mice. There were no differences at 17 and 21 DIV in prenode (i.e., Na_v and AnkG) clustering between *Nfasc*$^{-/-}$ and WT cultures (Fig. 5 and Fig. S4 *A* and *B*). Furthermore, when purified *Nfasc*$^{-/-}$ hippocampal neurons were cultured and treated with OCM, prenodal clustering was induced on GAD67^{+} neurons as in WT cultures (Fig. S4*C*). Therefore, the neuronal neurofascin isoform is not necessary for prenode assembly, and clustering of prenodes by OCM does not rely on an Nfasc186-based mechanism.

Prenode Assembly Requires AnkG. The cytoskeletal architecture has been seen to play an important role in the maintenance and possible clustering of the nodal complex (12, 18). We then addressed whether prenodal formation was dependent on AnkG by silencing AnkG expression within hippocampal cultures. Because AnkG is required for assembly and maintenance of the AIS (27, 28), transfection with either AnkG miRNA or control miRNA plasmids coexpressing GFP was performed at 6 DIV (i.e., after AIS assembly). In neurons expressing AnkG miRNA (GFP^{+}), AnkG was weakly detectable at the AIS, illustrating the efficiency of the miRNA (Fig. 6 *B* and *C*). Because AnkG removal may alter neuronal polarity (21), we analyzed Na_v clustering at a time point when microtubule associated protein 2 (MAP2) immunostaining was still restricted to the somatodendritic domain (Fig. 6*B*). In AnkG knockdown, GAD67^{+} neurons, some Na_v and Nfasc immunoreactivity was detected at the AIS, but Na_v clustering along the axon was completely prevented (Fig. 6 *A*, *C*, and *E* and Fig. S5). In contrast, in neurons transfected with the control plasmid, axonal clusters of AnkG, Na_v (Fig. 6 *D* and *E*), and Nfasc were formed.

Taken together, these results show that premyelination clustering of Na_v channels and Nfasc along axons of hippocampal neurons depends on AnkG.

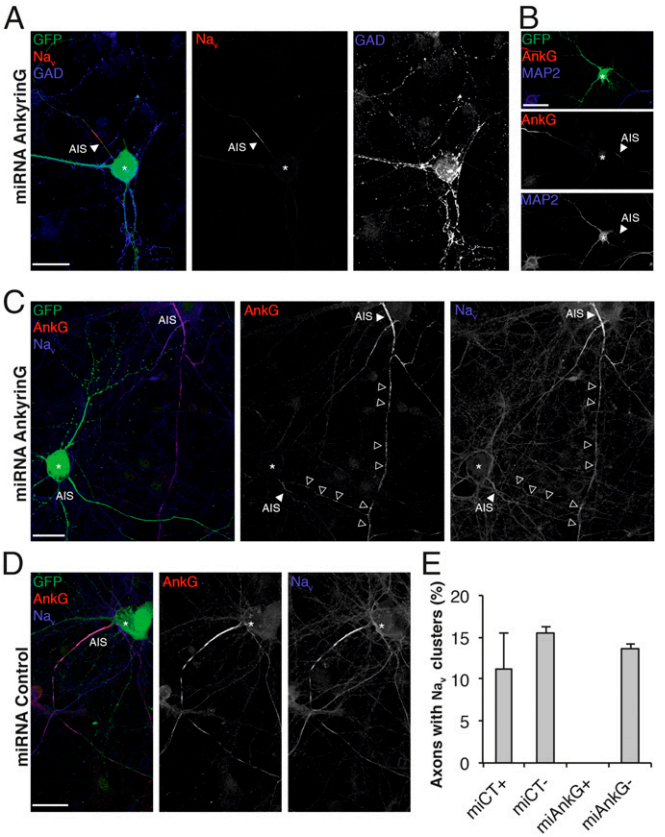

Fig. 6. Prenode assembly requires AnkG expression. (*A*–*C*) Immunostaining of hippocampal cell cultures transfected at 6 DIV with AnkG miRNA and fixed at 18 DIV. Transfected neurons are GFP^{+} (green). (*A*) Representative image of a transfected GAD67^{+} neuron (blue); Na_v expression (red) is weak at the AIS (arrowheads), and no prenodes are observed. (*B*) Transfected AnkG miRNA GFP^{+} neuron with somatodendritic expression of MAP2 (blue) and a weak AnkG (red) staining of the AIS (arrowheads). (*C*) Transfected AnkG miRNA GFP^{+} neuron with weak expression of AnkG (red) and Na_v (blue) at the AIS and no prenodes, whereas prenodes are observed in the neighboring nontransfected neuron (arrowheads). *Neuronal cell body. (*D*) Image of a neuron transfected with control miRNA showing AnkG (red) and Na_v (blue) expression at the AIS and prenodes. (*E*) Quantification of axons forming Na_v clusters in hippocampal cell cultures transfected (+) or not (–) with control miRNA (miCT) or AnkG miRNA (miAnkG). The means ± SDs of three independent experiments are shown. For each experiment, at least 50 neurons were analyzed. (Scale bars: 25 μm.)

Conduction Velocity Is Increased on Axons with Prenodes in the Absence of Myelination. We first investigated whether unmyelinated interneurons with and without prenodes had different intrinsic electrophysiological properties by performing somatic whole-cell patch-clamp recordings on mixed hippocampal cultures from *GAD67-GFP* knockin mice (29) (Fig. S6*A*). We observed no significant difference between the mean resting membrane potential, action potential (AP) threshold, AP rise time, AP half-width, and AP decay in cells with prenodes and those without (Fig. S6*B*). However, we observed that neurons with prenodes tended to exhibit a significantly lower input resistance compared to neurons without [with prenodes = 67.5 ± 24.5 MΩ; without prenodes = 175.1 ± 74.4 MΩ; $n = 7$ (each group); $P = 0.01$].

We then examined whether prenodal aggregates might accelerate axonal conduction velocity before myelination. Therefore, we compared electrical conduction on cultured rat mixed hippocampal GABAergic interneurons with and without prenodes using simultaneous recordings from the soma and axon of the same neuron from 10 to 19 DIV. AIS and prenodes were identified using live staining with an Ab targeting the extracellular domain of Nfasc (Fig. 7 *A* and *B*). Cell-attached patch-clamp recordings of action currents from the soma and axon were made during spontaneous firing of neurons at a minimum distance of 150 μm between the two recording electrodes (Fig. 7 *C* and *D*). At longer intervals between the somatic and axonal recording electrodes, we observed that the latencies between spikes recorded in the axon and at the soma increased in both neurons with and without prenodes (Fig. 7*E*). Interestingly, the mean apparent conduction velocity was significantly higher in neurons with prenodes compared to neurons without prenodes (Fig. 7*F*) (1.23 ± 0.09 m/s, $n = 10$; 0.72 ± 0.05 m/s, $n = 8$, respectively; $P = 0.0002$). Because the mean axonal diameter was significantly larger in neurons with prenodes compared to neurons without prenodes (1.96 ± 0.18 μm, $n = 10$; 1.26 ± 0.12 μm, $n = 8$, respectively; $P = 0.008$), one possibility might have been that increased conduction velocity was caused by larger axonal diameter. To test this alternative hypothesis, we selected neurons with and without prenodes having similar mean axonal diameters (1.71 ± 0.10 μm, $n = 3$; 1.68 ± 0.05 μm, $n = 3$, respectively) and showed that the mean conduction velocity was significantly higher in neurons with prenodes (1.24 ± 0.12 m/s, $n = 3$) compared to neurons without prenodes (0.74 ± 0.03 m/s, $n = 3$; $P = 0.016$). Taken together, these results show that clusters of nodal proteins increase axonal conduction velocity in hippocampal GABAergic neurons before myelination.

Prenodes Are Detected on Some Hippocampal GABAergic Neurons Before Myelination in Vivo. Using hippocampal tissue sections from *vesicular GABA transporter* (*VGAT*) *-venus* rat and *GAD67-GFP* mice (29, 30), we then addressed if this prenodal clustering occurred in vivo. We first showed that, in both rat and mouse CNS, some GABAergic neurons (GFP^+), mostly located in the stratum oriens of CA1 and CA3 and the subiculum (Fig. 8*A*), were myelinated as previously reported (31, 32). We then assessed whether prenodal clustering occurred at different premyelination time points. Indeed, axonal clusters of AnkG and Na_v channels were detected just before myelination (postnatal days P12 and P13) on some GABAergic neurons in the absence of myelin and paranodal accumulation of Caspr (Fig. 8 *B–E*). They had an intercluster interval ranging from 5 to 25 μm (seen in the plot profiles in Fig. 8 *B′*, *C′*, and *E′*), which is consistent with prenodes spacing measured on unmyelinated axons in vitro. These results show that prenode formation can occur before myelination in the hippocampus in vivo.

Discussion

Prenodal Clustering Occurs on GABAergic Interneurons in Vitro and in Vivo. Here, we report that discrete clusters of Na_v channels, colocalizing with AnkG and Nfasc, are detected before myelination along axons of hippocampal neurons in culture and during postnatal development in vivo. Notably, these clusters were detected on GABAergic neurons only and not on glutamatergic neurons, which constitute the other major subtype of hippocampal neurons. In the latter, nodal protein clustering coincides with myelination and paranodal junction formation. This result suggests that, depending on neuronal subtype, mechanisms of node of Ranvier formation can differ in the hippocampus and therefore, highlights the diversity of neuronal responses during development.

Interestingly, this restriction to a specific subtype was also seen when clustering was induced on purified hippocampal neurons by oligodendrocyte-conditioned media, strengthening the hypothesis that only neurons responsive to an oligodendroglial soluble signal form prenodes. What distinguishes neurons responsive and nonresponsive to this clustering signal is unknown. In this context, it is

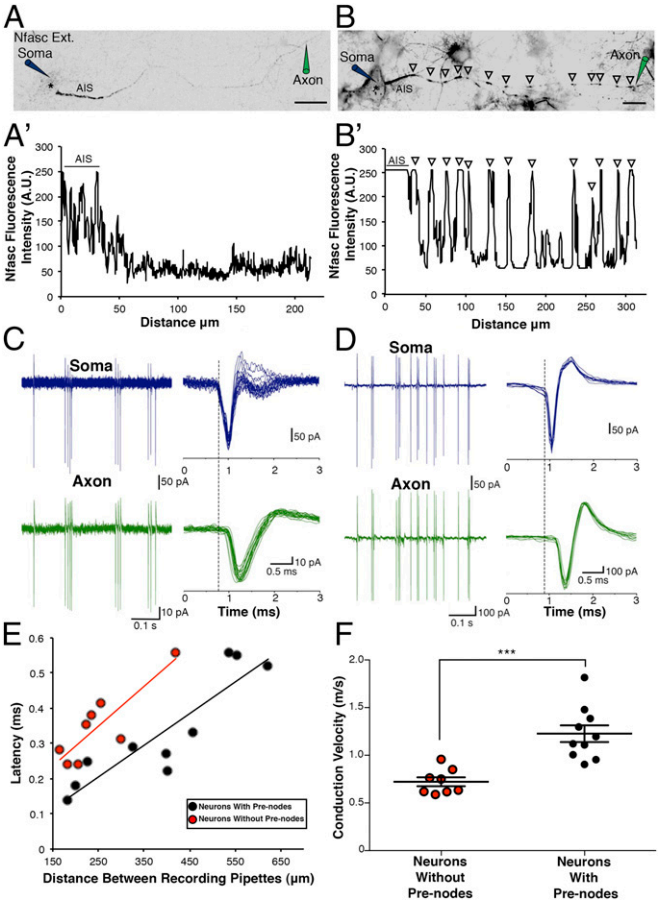

Fig. 7. Prenodes influence conduction velocity of unmyelinated neurons. (*A* and *B*) Live immunostaining of the AIS and prenodes (arrowheads) with an Ab recognizing the external domain of Nfasc and coupled to Alexa 594 during simultaneous recordings from the soma (blue-colored electrode) and axon (green-colored electrode) of neurons (*B*) with prenodes and (*A*) without prenodes in *VGAT-venus* rat hippocampal cultures. (Scale bar: 25 μm.) *Neuronal cell body. (*A′* and *B′*) Fluorescence intensity profiles corresponding to axonal Nfasc immunolabeling in *A* and *B*; individual peaks in *B′* correspond to prenodes (arrowheads), and fluorescence intensity is expressed in arbitrary units. (*C* and *D*) Spontaneous action currents recorded from the soma and axon from *A* and *B*, respectively. (*E*) Latencies plotted against recording distances (red points represent neurons without prenodes, and black points represent neurons with prenodes) show that latencies increase with recording distance ($R^2 = 0.737$, red line for neurons without prenodes; $R^2 = 0.801$, black line for neurons with prenodes). (*F*) Mean conduction velocity (CV) of neurons with prenodes is significantly increased compared with neurons without prenodes. CV for neuron in *A* = 0.85 m/s; CV for neuron in *B* = 1.12 m/s. ***$P = 0.0002$ (Student's *t* test).

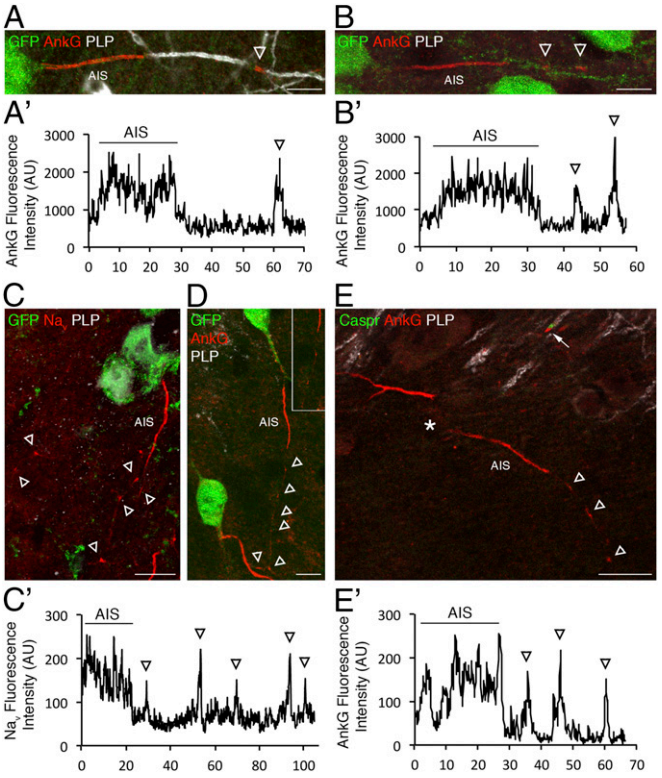

Fig. 8. Prenodes can be detected in vivo during postnatal development in both mouse and rat. (*A* and *B*) Immunostaining of sagittal sections of P13 *VGAT-venus* rat hippocampus shows the presence of AnkG$^+$ nodes of Ranvier on myelinated fibers (PLP$^+$) in *A* as well as AnkG axonal clusters in absence of myelin (PLP$^-$) in *B* on some GABAergic neurons stained with an anti-GFP Ab. (Scale bars: 10 μm.) Intensity profiles corresponding to AnkG expression in (*A′*) myelinated and (*B′*) nonmyelinated fibers. Arrowheads indicate AnkG axonal clusters. (*C* and *D*) Immunostaining of sagittal sections of P12 *GAD-GFP* mouse hippocampus shows the presence of (*C*) Na$_v$ and (*D*) AnkG clusters (arrowheads) in the absence of myelin (PLP$^-$). In *D*, the boxed area is shown as a zoomed-in view. (Scale bars: 10 μm.) (*E*) Immunostaining of P12 *GAD-GFP* hippocampus shows that Caspr is not clustered around prenodal AnkG before myelination (arrowheads), whereas it is accumulated at hemiparanodes flanking nodal AnkG in myelinated fibers (arrow). *Neuronal cell body. (Scale bar: 20 μm.) (*C′* and *E′*) Intensity profiles corresponding to (*C*) Na$_v$ staining and (*D*) AnkG show isolated peaks corresponding to prenodes (arrowheads).

of note that the induction of Na$_v$ clustering by a soluble oligodendroglial factor has been identified previously by Kaplan et al. (20, 21) on RGCs, which are glutamatergic neurons, suggesting that the clustering permissivity does not depend on the type of neurotransmitter. An attractive hypothesis is that prenodal formation might be associated with the need for early establishment of neuronal connections during development on axons with long trajectories. In favor of this hypothesis, these two types of axons with prenodes are known to be characterized by long-range projecting axons: RGC axons extend from the retina to the superior colliculus, and our results reveal that most axons with clusters in vivo extended from the CA1 region of the hippocampus, which has been found to project to farther interregional areas, such as the medial septum, the subiculum, or the retrosplenial cortex (31, 33, 34).

Lastly, whether these nodal protein clusters disappear or fuse to form nodes of Ranvier when oligodendrocyte processes contact the axon, such as described for heminodes (35, 36), remains to be determined. Indeed, the increase in the spacing of nodal clusters upon myelination in vitro and in vivo along GABAergic axons suggests that spatial rearrangements could occur.

Oligodendrocyte-Secreted Factor Induces Prenodal Clustering. Our results on purified hippocampal neurons extend previous data that a proteinaceous factor(s) secreted by oligodendroglia induces clustering of nodal proteins (20, 21). Whether this factor(s) induces Na$_v$ clustering through interactions with the axonal membrane or stimulation of neuronal protein synthesis has yet to be fully understood. Gliomedin expressed by Schwann cells is known to induce nodal clustering in the peripheral nervous system (7). However, not only has CNS expression of gliomedin not been reported, but also, we found that gliomedin was undetectable both in oligodendroglial cultures and at prenodes. The various ECM proteins enriched at the CNS nodes mainly play a role in buffering nodal environment and stabilizing the nodes (10–12). Whether they participate in the induction of prenodal assembly remains to be seen. However, our results provide that clustering of prenodes through OCM is not mediated through an Nfasc-based mechanism, implying that other cell adhesion molecules may interact with the oligodendroglial-secreted factor. Furthermore, we addressed whether this oligodendroglial clustering effect might be related to oligodendrocyte-induced neuronal maturation and survival (37). This hypothesis was partly supported by the facts that clusters were mostly detected in vitro on large-diameter axons with highly phosphorylated neurofilaments, a hallmark of maturation, that also, in vivo, prenodes were found more frequently at P12 and P13 compared with earlier time points, and lastly, that neurons with prenodes exhibited a lower input resistance compared to neurons without clusters. In accordance with these findings, it has been observed that there is a significant decrease in the input resistance as mice matured from P9–P11 to P12–P16 (38). However, addition of maturation/growth factors [glial cell derived neurotrophic factor (GDNF), BDNF, ciliary neurotrophic factor (CNTF), leukemia inhibitory factor (LIF), or NGF] to pure neuron cultures while inducing neurofilament phosphorylation did not trigger Na$_v$ clustering, suggesting that axonal maturation is not sufficient to induce nodal protein clustering. We also addressed the role of electrical activity by using tetrodotoxin or veratridine (blocker and activator of Na$_v$ channels, respectively), which did not affect prenode formation.

AnkG Is Essential for Prenodal Formation, Whereas Nfasc Is Dispensable. In the CNS, several mechanisms are involved in nodal assembly: clustering of Nfasc186 through interactions with ECM, restriction of diffusion through paranodal junctions, and stabilization by the cytoskeletal scaffold. Numerous studies suggest that these three mechanisms are alternative or complementary to induce nodal assembly (8, 9). Direct axoglial contacts established at the paranodal junctions have been suggested to induce nodal protein clustering through restriction of their diffusion (12, 13). Nevertheless, other studies have indicated that, when paranode assembly is impaired by inactivation of genes coding for the paranodal proteins (Caspr, contactin, or Nfasc155) or the myelin proteins, the timing and number of developing nodes occur normally, suggesting that formation of paranodal junctions may be sufficient but not necessary for nodal assembly (14–19). Recently, by using a genetic strategy to determine their requirement, Susuki et al. (12) have shown that disruption of at least two of these three mechanisms is necessary to affect node formation. We show here that Na$_v$ clusters can be formed without direct axoglial contact, which has been previously found (20, 21). We also show that AnkG is required for the formation of Na$_v$ and Nfasc186 clusters along unmyelinated axons. AnkG, which likely provides a link by establishing interactions with the intracellular domains of Nfasc186 and Na$_v$ α-subunit as well as βIV spectrin and kinesin motors (39, 40), may either initiate or stabilize prenodal protein clustering before myelination. In contrast, Nfasc is not necessary for Na$_v$ and AnkG prenodal clustering. This result suggests that Nfasc186 plays a role in late rather than early stages of node of Ranvier assembly.

Na_v Clustering Is Differentially Regulated in Prenodes. We observed that distinct Na_v channel isoforms are targeted differentially in prenodes along different time points in vitro. Whereas the $Na_v1.1$ isoform is found at all time points, the immature isoform $Na_v1.2$ progressively disappears, and $Na_v1.6$ is recruited in ∼35% of neurons with prenodes in mixed culture. One noteworthy finding is that $Na_v1.6$ was found in the absence of myelination, but $Na_v1.6$ does not appear in axonal clusters on purified hippocampal neurons treated with OCM, the latter of which are similar to those previously reported on purified RGCs treated with OCM (21). Interestingly, the timing of $Na_v1.6$ expression at prenodes coincided with late in vitro culture time points, wherein its first appearance started at 17 DIV and gradually increased up to 24 DIV. These results may implicate either the transition of immature to mature oligodendrocytes in culture and/or that neuronal maturation is necessary to synthesize and recruit $Na_v1.6$ to prenodes. Although these results differ from a previous report of $Na_v1.6$ recruitment requiring myelin compaction during optic nerve development (25), these results nevertheless point to an important role for the physical presence of oligodendrocytes to target $Na_v1.6$ at prenodes. Because we did observe some CNP-EGFP$^+$ oligodendrocytes contacting prenodal clusters, it would be interesting to investigate the role of oligodendroglial contact and their influence on the distribution of sodium channel subtypes, which may shed light onto additional cues necessary for $Na_v1.6$ targeting in the CNS.

What Are the Functional Roles of Prenodes? What is the functional gain provided by axonal Na_v clusters in the absence of myelin? Axonal propagation velocity of the action potential is known to depend on the axon diameter and the presence of a myelin sheath (41). Here, our whole-cell patch-clamp recordings and single-axon electrophysiological results strongly suggest that the presence of regularly spaced Na_v clusters increases action potential propagation in the absence of myelination independent of axonal caliber, and these data suggest another level of influence by oligodendrocytes on the regulation of conduction velocity beyond the production of a myelin sheath. In addition, the shorter interval between prenodes compared with mature nodes of Ranvier could compensate for a lack of insulation in the absence of myelin. Of note, on GABAergic neurons with prenodal clusters, recorded apparent conduction velocities were in a similar range to those reported for myelinated axons of cortical pyramidal neurons (42, 43). Prenodes with high-density sodium channel clusters could serve as acceleration points, which was predicted by theoretical modeling calculations (44, 45). It is tempting to speculate that optimization of propagation of electrical signaling at a given developmental stage will be especially crucial for highly connected GABAergic hub neurons, which have a widespread axonal arborization, and for long-range projection neurons, and provides a means to impact network activities (33). Moreover, Na_v clustering may help to overcome axonal branch point failures and maintain reliable propagation of action potentials (41).

In multiple sclerosis, within lesions undergoing remyelination, clustering of Na_v channels has been observed on PLP$^-$ (i.e., nonremyelinated) fibers (46), suggesting that, such as for developmental myelination, nodal protein clustering might precede myelin repair. Although the mechanisms of axonal domain reassembly during remyelination are still poorly understood, it can be hypothesized that, similar to early nodal clustering during developmental myelination, these clusters accelerate conduction velocity before remyelination and therefore, participate in functional recovery.

Materials and Methods

Animals. The care and use of rats and mice in all experiments conformed to institutional policies and guidelines (UPMC, INSERM, and European Community Council Directive 86/609/EEC). The following rat and mouse strains were used in this study: Sprague–Dawley or Wistar rats (Janvier Breeding Center), *VGAT-venus* Wistar rats (30), *Nfasc*$^{-/-}$ mice (1), *GAD67-GFP* knockin mice (29), *CNP-EGFP* mice (24), and C57bl/6 WT mice.

Cell Cultures. Mixed hippocampal cultures (containing neurons and glial cells) at E18 were prepared according to procedures described previously (47) with modifications. Briefly, pooled hippocampi were dissociated enzymatically by trypsin (0.1%; Worthington) treatment for 20 min with DNase (50 μg/mL). After trypsin neutralization, cells were centrifuged at 400 × *g* for 5 min, resuspended, and then seeded on polyethylenimine precoated glass coverslips at a density of 5.0×10^4 cells/35 mm^2. Cultures were maintained for 24 h in a 1:1 mixture of DMEM (11880; Gibco) with 10% FCS (100 IU/mL), penicillin-streptomycin (100 IU/mL), and neuron culture medium (NCM). Culture medium was replaced by a 1:1 mixture of Bottenstein–Sato (BS) medium with PDGF-A (0.5%) and NCM, and then, one-half of the medium was changed every 3 d and replaced by NCM. To increase myelination in cultures maintained until 24–28 DIV, differentiation medium was added at 18 DIV. Compositions of NCM, BS medium, and differentiation medium are detailed in *SI Materials and Methods*. Purified hippocampal neuronal cultures were obtained by adding (24 h after isolation) the antimitotic agents uridine and 5-fluorodeoxyuridine (5 μM; Sigma) to the NCM for 36 h. Cultures of dopaminergic neurons were prepared from Wistar rats at E15.5 according to procedures described previously (48). Glial cell cultures were prepared using cerebral cortices from P2 Wistar rats dissected free of meninges, then incubated for 45 min in papain (30 U/mL; Worthington) supplemented with L-cysteine (0.24 mg/mL) and DNase (50 μg/mL) in DMEM at 37 °C, and mechanically homogenized. Cells were resuspended in DMEM with 10% FCS and penicillin-streptomycin and dispensed into T175 culture flasks at a density of 10^5 cells/cm^2. After 12–15 d in culture, flasks were shaken for 1 h at 180 rpm to remove microglial cells, medium was replaced, and flasks were shaken on a rotary shaker overnight at 230 rpm at 37 °C. Detached cells were used for immunopanning (*SI Materials and Methods*) to isolate oligodendrocytes. All cultures were maintained at 37 °C and 5% CO_2.

Preparation of OCM. Oligodendrocytes were cultured for 24 h in BS medium, and then, medium was replaced with NCM and collected after 48 h. OCM was filtered through a 0.22-μm filter. Protein concentration (4.1 ± 2.4 μg/μL, mean ± SD of four OCMs) was measured using the bicinchoninic acid (BCA) protein assay (Pierce).

Purified Hippocampal Neurons Cultured with OCM or Oligodendrocytes. OCM (500 μL/well) or oligodendrocytes (2.5×10^4 cells/well) were added to purified hippocampal neuronal cultures at 3 DIV after removal of antimitotic agents. Then, one-half of the medium was changed with NCM every 5 d. Percentages of neurons (AnkG$^+$ cells), astrocytes (GFAP$^+$ cells), and oligodendrocytes (O4$^+$ and PLP$^+$ cells) were determined at 21 DIV. Mixed hippocampal cultures contained 43.7% ± 2.7% of neurons, 42.5% ± 5.4% of astrocytes, and 11.2% ± 2.7% of oligodendrocytes, whereas purified neuronal cultures contained 94.2% ± 2.2% of neurons, 3.6% ± 1.7% of astrocytes, and 0.4% ± 0.6% of oligodendrocytes; purified neurons cultured with OCM contained 92% ± 2.6% of neurons, 4.3% ± 3.4% of astrocytes, and 0.5% ± 0.5% of oligodendrocytes; and purified neurons cocultured with oligodendrocytes contained 77.5% ± 3.5% of neurons, 4.5% ± 4.2% of astrocytes, and 17.3% ± 0.4% of oligodendrocytes (mean ± SD; $n = 3$, 150 cells at least were counted for each experiment).

Tissue Sections. *GAD67-GFP* mice and *VGAT-venus* rats were anesthetized at P12 and P13 with lethal doses of Imalgen 500 (Merial) combined with 2% Rompun (Bayer). They were transcardially perfused with 1% or 4% paraformaldehyde (PFA), and brains were dissected and postfixed in 1% or 4% PFA followed by PBS washes and subsequent equilibration in sucrose (5–30%) solution overnight at 4 °C for cryostat sectioning. The next day, brains were embedded in OCT (Tissue-Tek), frozen, and then cryosectioned (CM 3050; Leica) at 35 μm. Serial sectioning of the hippocampus was in the sagittal plane.

Abs and Immunofluorescence. All Abs used can be found listed in *SI Materials and Methods*. Cell cultures were fixed with 4% PFA for 10 min or for Na_v channel staining, 1% PFA for 10 min at room temperature (RT) and then incubated with methanol for 10 min at −20 °C. Coverslips were then washed with PBS one time. After fixation, cells were incubated with blocking buffer (BB; 1× PBS, 5% normal goat serum, 0.1% Triton) for 15 min and then primary Ab (diluted in BB) for 2 h at RT or 4 °C overnight. Coverslips were then washed and incubated with secondary Ab at RT for 1 h. After last wash, Hoechst stain (1 mM) was placed on cells at RT for 5 min. Floating brain cryostat sections were pretreated with ethanol at −20 °C for 10 min and then washed with PBS. They were then treated with BB with 0.2% Triton for 1 h at RT before incubation with Ab overnight at 4 °C. Sections were then washed, and secondary Abs were added for 2 h at RT. Coverslips and sections were mounted on superfrost glass slides with Fluoromount G (Southern Biotech).

Image Acquisition and Analysis. Slides from hippocampal cultures and cryostat sections were visualized using an Olympus FV-1000 Upright Confocal Microscope or a Zeiss AxioImager-Apotome. *Z* series of optical sections was performed at 0.3-μm increments for qualitative analysis. Blue, green, red, and far-red fluorescence was acquired sequentially. Maximum orthogonal projection of images and plot profiles of immunofluorescence intensity were carried out using ImageJ software (NIH).

Quantification of Neurons with Clusters, Sizes of Clusters, Intervals, and Myelination. At least 100 neurons per coverslip, identified by the presence of an AIS, were counted, and the percentage of neurons with Na_v/AnkG clusters was determined for at least two coverslips per condition. Results were expressed as means ± SDs of at least three independent experiments. An Na_v cluster was defined by its size and mean intensity of area (i.e., size of clusters varied from 1 to 8 μm, and mean value of cluster area was at least 2.5 that of the adjacent part of the axon). Intervals between clusters were measured on acquired images by using ImageJ software. The mean intervals were calculated for one neuron; then, the mean of all neurons for one experiment was determined, and results were expressed as means ± SEMs of four independent experiments. Myelination was assessed at 24 DIV and identified as bright PLP^+ double lines interrupted at nodes of Ranvier. Statistical analyses were performed using the Mann–Whitney test or Student's *t* test with Prism software (GraphPad software).

Design and Transfection of miRNA. To generate AnkG miRNA constructs, we used the Block-it PolII miR RNAi Expression Vector Kits (K4936-00) (*SI Materials and Methods*). Hippocampal cells in 24-well plates were transfected at 6 DIV with 0.5 μg DNA/well using the lipofectamine 2000 reagent according to the manufacturer's protocol (11668–019; Invitrogen). Transfected cells were fixed at 18 or 20 DIV. The two miRNAs used gave similar results.

Electrophysiology: Simultaneous Soma/Axon Recordings. Rat hippocampal cultures were used between 10 and 19 DIV for electrophysiological recordings. Nfasc external Ab (cloneA12/18; Neuromab) was coupled to Alexa 594 according to the manufacturer's protocol (A10474; Invitrogen) and then incubated on hippocampal cultures for 30 min at 37 °C with a 1:15 dilution in culture medium. Labeled cultures were transferred to the recording chamber on the stage of an Axioskop 2 FS plus microscope (Zeiss) and continuously superfused with artificial cerebrospinal fluid. Simultaneous patch recordings were performed with a Multiclamp 700B amplifier (Molecular Devices) and digitized with pClamp10 software (Axon; Molecular Devices). Spontaneous action currents were recorded in cell-attached mode from both the somatic and axonal electrodes (*SI Materials and Methods*).

ACKNOWLEDGMENTS. We thank François Couraud, Rock Levinson, and Elior Peles for the gift of Abs. We also thank Bernard Zalc, Charles-Felix Calvo, and members of the laboratory of C.L. for discussions and critical reading of the manuscript. We thank Plate-forme d'Imagerie Cellulaire de la Pitié-Salpêtrière for support with image acquisition. This work was supported by INSERM, French Multiple Sclerosis Research Foundation association pour la recherche sur la sclérose en plaques (ARSEP) Program "Investissements d'avenir" ANR-10-IAIHU-06, and the Bouvet–Labruyère prize (to N.S.-F.). S.A.F. and A.D. were supported by the French Medical Research Foundation, and C.L. was supported by the Sobeck Prize. P.J.B. was supported by the Wellcome Trust.

1. Sherman DL, Brophy PJ (2005) Mechanisms of axon ensheathment and myelin growth. *Nat Rev Neurosci* 6(9):683–690.
2. Charles P, et al. (2002) Neurofascin is a glial receptor for the paranodin/Caspr-contactin axonal complex at the axoglial junction. *Curr Biol* 12(3):217–220.
3. Sherman DL, et al. (2005) Neurofascins are required to establish axonal domains for saltatory conduction. *Neuron* 48(5):737–742.
4. Lustig M, et al. (2001) Nr-CAM and neurofascin interactions regulate ankyrin G and sodium channel clustering at the node of Ranvier. *Curr Biol* 11(23):1864–1869.
5. Zhang Y, et al. (2012) Assembly and maintenance of nodes of ranvier rely on distinct sources of proteins and targeting mechanisms. *Neuron* 73(1):92–107.
6. Feinberg K, et al. (2010) A glial signal consisting of gliomedin and NrCAM clusters axonal Na+ channels during the formation of nodes of Ranvier. *Neuron* 65(4):490–502.
7. Eshed Y, et al. (2005) Gliomedin mediates Schwann cell-axon interaction and the molecular assembly of the nodes of Ranvier. *Neuron* 47(2):215–229.
8. Chang KJ, Rasband MN (2013) Excitable domains of myelinated nerves: Axon initial segments and nodes of Ranvier. *Curr Top Membr* 72(2013):159–192.
9. Leterrier C, Brachet A, Dargent B, Vacher H (2011) Determinants of voltage-gated sodium channel clustering in neurons. *Semin Cell Dev Biol* 22(2):171–177.
10. Dours-Zimmermann MT, et al. (2009) Versican V2 assembles the extracellular matrix surrounding the nodes of ranvier in the CNS. *J Neurosci* 29(24):7731–7742.
11. Bekku Y, Rauch U, Ninomiya Y, Oohashi T (2009) Brevican distinctively assembles extracellular components at the large diameter nodes of Ranvier in the CNS. *J Neurochem* 108(5):1266–1276.
12. Susuki K, et al. (2013) Three mechanisms assemble central nervous system nodes of Ranvier. *Neuron* 78(3):469–482.
13. Rasband MN, et al. (1999) Dependence of nodal sodium channel clustering on paranodal axoglial contact in the developing CNS. *J Neurosci* 19(17):7516–7528.
14. Mathis C, Denisenko-Nehrbass N, Girault JA, Borrelli E (2001) Essential role of oligodendrocytes in the formation and maintenance of central nervous system nodal regions. *Development* 128(23):4881–4890.
15. Bhat MA, et al. (2001) Axon-glia interactions and the domain organization of myelinated axons requires neurexin IV/Caspr/Paranodin. *Neuron* 30(2):369–383.
16. Boyle ME, et al. (2001) Contactin orchestrates assembly of the septate-like junctions at the paranode in myelinated peripheral nerve. *Neuron* 30(2):385–397.
17. Ishibashi T, et al. (2002) A myelin galactolipid, sulfatide, is essential for maintenance of ion channels on myelinated axon but not essential for initial cluster formation. *J Neurosci* 22(15):6507–6514.
18. Jenkins SM, Bennett V (2002) Developing nodes of Ranvier are defined by ankyrin-G clustering and are independent of paranodal axoglial adhesion. *Proc Natl Acad Sci USA* 99(4):2303–2308.
19. Zonta B, et al. (2008) Glial and neuronal isoforms of Neurofascin have distinct roles in the assembly of nodes of Ranvier in the central nervous system. *J Cell Biol* 181(7):1169–1177.
20. Kaplan MR, et al. (1997) Induction of sodium channel clustering by oligodendrocytes. *Nature* 386(6626):724–728.
21. Kaplan MR, et al. (2001) Differential control of clustering of the sodium channels Na(v)1.2 and Na(v)1.6 at developing CNS nodes of Ranvier. *Neuron* 30(1):105–119.
22. Freund TF, Buzsáki G (1996) Interneurons of the hippocampus. *Hippocampus* 6(4):347–470.
23. Jinno S, Kosaka T (2000) Colocalization of parvalbumin and somatostatin-like immunoreactivity in the mouse hippocampus: Quantitative analysis with optical dissector. *J Comp Neurol* 428(3):377–388.
24. Yuan X, et al. (2002) Expression of the green fluorescent protein in the oligodendrocyte lineage: A transgenic mouse for developmental and physiological studies. *J Neurosci Res* 70(4):529–545.
25. Boiko T, et al. (2001) Compact myelin dictates the differential targeting of two sodium channel isoforms in the same axon. *Neuron* 30(1):91–104.
26. Duflocq A, Le Bras B, Bullier E, Couraud F, Davenne M (2008) Nav1.1 is predominantly expressed in nodes of Ranvier and axon initial segments. *Mol Cell Neurosci* 39(2):180–192.
27. Hedstrom KL, et al. (2007) Neurofascin assembles a specialized extracellular matrix at the axon initial segment. *J Cell Biol* 178(5):875–886.
28. Hedstrom KL, Ogawa Y, Rasband MN (2008) AnkyrinG is required for maintenance of the axon initial segment and neuronal polarity. *J Cell Biol* 183(4):635–640.
29. Tamamaki N, et al. (2003) Green fluorescent protein expression and colocalization with calretinin, parvalbumin, and somatostatin in the GAD67-GFP knock-in mouse. *J Comp Neurol* 467(1):60–79.
30. Uematsu M, et al. (2008) Quantitative chemical composition of cortical GABAergic neurons revealed in transgenic venus-expressing rats. *Cereb Cortex* 18(2):315–330.
31. Jinno S, et al. (2007) Neuronal diversity in GABAergic long-range projections from the hippocampus. *J Neurosci* 27(33):8790–8804.
32. Meier S, Bräuer AU, Heimrich B, Nitsch R, Savaskan NE (2004) Myelination in the hippocampus during development and following lesion. *Cell Mol Life Sci* 61(9):1082–1094.
33. Picardo MA, et al. (2011) Pioneer GABA cells comprise a subpopulation of hub neurons in the developing hippocampus. *Neuron* 71(4):695–709.
34. Melzer S, et al. (2012) Long-range-projecting GABAergic neurons modulate inhibition in hippocampus and entorhinal cortex. *Science* 335(6075):1506–1510.
35. Vabnick I, Novaković SD, Levinson SR, Schachner M, Shrager P (1996) The clustering of axonal sodium channels during development of the peripheral nervous system. *J Neurosci* 16(16):4914–4922.
36. Custer AW, et al. (2003) The role of the ankyrin-binding protein NrCAM in node of Ranvier formation. *J Neurosci* 23(31):10032–10039.
37. Du Y, Dreyfus CF (2002) Oligodendrocytes as providers of growth factors. *J Neurosci Res* 68(6):647–654.
38. Holter NI, Zuber N, Bruehl C, Draguhn A (2007) Functional maturation of developing interneurons in the molecular layer of mouse dentate gyrus. *Brain Res* 1186:56–64.
39. Bennett V, Baines AJ (2001) Spectrin and ankyrin-based pathways: Metazoan inventions for integrating cells into tissues. *Physiol Rev* 81(3):1353–1392.
40. Barry J, et al. (2014) Ankyrin-G directly binds to kinesin-1 to transport voltage-gated Na+ channels into axons. *Dev Cell* 28(2):117–131.
41. Debanne D, Campanac E, Bialowas A, Carlier E, Alcaraz G (2011) Axon physiology. *Physiol Rev* 91(2):555–602.
42. Palmer LM, Stuart GJ (2006) Site of action potential initiation in layer 5 pyramidal neurons. *J Neurosci* 26(6):1854–1863.
43. Popovic MA, Foust AJ, McCormick DA, Zecevic D (2011) The spatio-temporal characteristics of action potential initiation in layer 5 pyramidal neurons: A voltage imaging study. *J Physiol* 589(Pt 17):4167–4187.
44. Johnston WL, Dyer JR, Castellucci VF, Dunn RJ (1996) Clustered voltage-gated Na+ channels in Aplysia axons. *J Neurosci* 16(5):1730–1739.
45. Zeng S, Tang Y (2009) Effect of clustered ion channels along an unmyelinated axon. *Phys Rev E Stat Nonlin Soft Matter Phys* 80(2 Pt 1):021917.
46. Coman I, et al. (2006) Nodal, paranodal and juxtaparanodal axonal proteins during demyelination and remyelination in multiple sclerosis. *Brain* 129(Pt 12):3186–3195.
47. Banker GA, Cowan WM (1977) Rat hippocampal neurons in dispersed cell culture. *Brain Res* 126(3):397–445.
48. Toulorge D, et al. (2011) Neuroprotection of midbrain dopamine neurons by nicotine is gated by cytoplasmic Ca2+. *FASEB J* 25(8):2563–2573.